

Contents lists available at SciVerse ScienceDirect

Journal of Sound and Vibration

journal homepage: www.elsevier.com/locate/jsvi



Stable methods to solve the impedance matrix for radially inhomogeneous cylindrically anisotropic structures

Andrew N. Norris, Adam J. Nagy*, Feruza A. Amirkulova

Mechanical and Aerospace Engineering, Rutgers University, Piscataway, NJ 08854, United States

ARTICLE INFO

Article history: Received 2 July 2012 Received in revised form 15 December 2012 Accepted 19 December 2012 Handling Editor: G. Degrande Available online 26 January 2013

ABSTRACT

A stable approach for integrating the impedance matrix in cylindrical, radial inhomogeneous structures is developed and studied. A Stroh-like system using the time-harmonic displacement-traction state vector is used to derive the Riccati matrix differential equation involving the impedance matrix. It is found that the resulting equation is stiff and leads to exponential instabilities. A stable scheme for integration is found in which a local expansion is performed by combining the matricant and impedance matrices. This method offers a stable solution for fully anisotropic materials, which was previously unavailable in the literature. Several approximation schemes for integrating the Riccati equation in cylindrical coordinates are considered: exponential, Magnus, Taylor series, Lagrange polynomials, with numerical examples indicating that the exponential scheme performs best. The impedance matrix is compared with solutions involving Buchwald potentials in which the material is limited to piecewise constant transverse isotropy. Lastly a scattering example is considered and compared with the literature.

© 2013 Published by Elsevier Ltd.

1. Introduction

Wave propagation in layered elastic media has been widely studied resulting in a variety of solution approaches. These include the use of scalar and vector potentials [1], the transfer matrix method [2–6], and the delta matrix method [7,8]. Alternatively, computationally stable methods have also been developed, e.g. the stiffness matrix [9,10], the global matrix [11], and the reflectivity method [12]. Such approaches are limited to isotropic or transversely isotropic materials whereas we are interested in general anisotropic solids in order to develop scattering solutions related to metamaterial devices such as acoustic cloaks [13–15] which can be modeled as radially inhomogeneous anisotropic solids. The goal of this paper is to produce a stable solution method for such materials.

We considered a matricant propagator solution [16,17] based on the Stroh formalism to solve for scattering from a generally anisotropic material. The method involves the creation of a state space representation of the system where six first order, ordinary differential equations, must be integrated which may often diverge. A stable scheme for finding the solution to the differential equations, inspired by [18], is developed by combining the matricant and impedance matrices. The scheme is considered with several different expansion methods to yield relatively high orders of accuracy and is compared with solutions from the conditional impedance matrix and Buchwald's scalar potentials [19].

The outline of the paper is as follows. In Section 2, we begin with definitions of the impedance and matricant matrices. An explicit method for finding the impedance in piecewise uniform, transversely isotropic materials is developed in Section 3. This method also serves as a tool to compare with more general solution methods based on the Riccati matrix differential equation for the impedance matrix. It is found that the Riccati differential equation is stiff and leads to exponentially growing

E-mail addresses: norris@rutgers.edu (A.N. Norris), adnagy@eden.rutgers.edu (A.J. Nagy), feruza@eden.rutgers.edu (F.A. Amirkulova).

^{*}Corresponding author. Tel.: +1 908 279 3863.

instabilities. In Section 4, an alternative approach for integrating the matricant is derived to find a stable means of integrating the impedance matrix. We then use different expansion techniques used in the integration process in order to find higher order accurate schemes. Lastly in Section 5 a scattering example from the literature is considered.

2. Impedance and matricant matrices

We consider time harmonic wave motion in radially inhomogeneous cylindrically anisotropic solids. The associated equilibrium equations for linear elastodynamics in cylindrical coordinates are summarized in Appendix A. Here we need only focus on the relation between the vectors $\mathbf{U}(r)$ and $\mathbf{V}(r)$ associated with displacement and traction, respectively. Precise definitions follow from Eqs. (A.5) (which includes the superscript n that is omitted here for simplicity). The dimension of each vector is taken as m, where m is either 3, 2 or 1; m=3 in general, m=2 if z-dependence is not considered, and m=1 for pure out-of-plane shear horizontal (SH) motion. For the moment we may consider m as general. The main focus of the paper is the $m \times m$ conditional impedance matrix \mathbf{z} defined such that

$$\mathbf{V}(r) = -i\mathbf{z}(r)\mathbf{U}(r). \tag{1}$$

It is shown in Eq. (A.6) that the equations for linear elastodynamics can be cast as a system of 2m linear ordinary differential equations [17]

$$\frac{\mathrm{d}\boldsymbol{\eta}}{\mathrm{d}r} = \mathbf{Q}\boldsymbol{\eta} \quad \text{with } \boldsymbol{\eta}(r) = \begin{pmatrix} \mathbf{U} \\ \mathbf{V} \end{pmatrix}, \quad \mathbf{Q}(r) = \begin{pmatrix} \mathbf{Q}_1 & \mathbf{Q}_2 \\ \mathbf{Q}_3 & \mathbf{Q}_4 \end{pmatrix}, \tag{2}$$

where $\mathbf{Q}^+ = -\mathbf{T}\mathbf{Q}\mathbf{T}$, $^+$ denotes the Hermitian transpose and \mathbf{T} is defined in (A.10). It follows from Eqs. (1) and (2) that $\mathbf{z}(r)$ satisfies a differential Riccati equation

$$\frac{d\mathbf{z}}{d\mathbf{r}} + \mathbf{z}\mathbf{Q}_1 - \mathbf{Q}_4\mathbf{z} - i\mathbf{z}\mathbf{Q}_2\mathbf{z} - i\mathbf{Q}_3 = \mathbf{0},\tag{3}$$

with assumed initial condition $\mathbf{z}(r_0)$ at some specified $r = r_0$, hence the name conditional impedance.

One approach to solving for the conditional impedance matrix, \mathbf{z} , is to first solve for the $2m \times 2m$ matricant $\mathbf{M}(r,r_0)$ which is defined as the solution of the initial value problem

$$\frac{d\mathbf{M}}{dr}(r,r_0) = \mathbf{Q}(r)\mathbf{M}(r,r_0), \quad \mathbf{M}(r_0,r_0) = \mathbf{I}_{(2m)}, \quad \mathbf{M} = \begin{pmatrix} \mathbf{M}_1 & \mathbf{M}_2 \\ \mathbf{M}_3 & \mathbf{M}_4 \end{pmatrix}. \tag{4}$$

Hence

$$\mathbf{\eta}(r) = \mathbf{M}(r, r_0)\mathbf{\eta}(r_0). \tag{5}$$

Using the relations

$$\mathbf{U}(r) = (\mathbf{M}_1 - i\mathbf{M}_2 \mathbf{z}(r_0))\mathbf{U}(r_0), \quad \mathbf{V}(r) = (\mathbf{M}_3 - i\mathbf{M}_4 \mathbf{z}(r_0))\mathbf{U}(r_0), \tag{6}$$

which follow from (1), the conditional impedance can be expressed in terms of the matricant as

$$\mathbf{z}(r) = \mathrm{i}(\mathbf{M}_3 - \mathrm{i}\mathbf{M}_4 \mathbf{z}(r_0))(\mathbf{M}_1 - \mathrm{i}\mathbf{M}_2 \mathbf{z}(r_0))^{-1}. \tag{7}$$

The propagator nature of the matricant is apparent from Eq. (5) and from the property $\mathbf{M}(r,r_1)$ $\mathbf{M}(r_1,r_0) = \mathbf{M}(r,r_0)$, and in particular $\mathbf{M}(r,r_0) = \mathbf{M}(r_0,r)^{-1}$. Also, the symmetry (A.10) implies $\mathbf{M}(r,r_0) = \mathbf{T}\mathbf{M}^+(r_0,r)\mathbf{T}$. Hence, $\mathbf{M}^{-1}(r,r_0) = \mathbf{T}\mathbf{M}^+(r,r_0)\mathbf{T}$, that is, \mathbf{M} is \mathbf{T} -unitary [20].

An alternative approach to finding z uses the two-point impedance matrix, which by definition relates the traction and displacement vectors at two values of r according to [17]

$$\begin{pmatrix} \mathbf{V}(r_0) \\ -\mathbf{V}(r) \end{pmatrix} = -i\mathbf{Z}(r, r_0) \begin{pmatrix} \mathbf{U}(r_0) \\ \mathbf{U}(r) \end{pmatrix}, \quad \mathbf{Z} = \begin{pmatrix} \mathbf{Z}_1 & \mathbf{Z}_2 \\ \mathbf{Z}_3 & \mathbf{Z}_4 \end{pmatrix}. \tag{8}$$

The two-point impedance matrix has the important property that it is Hermitian, $\mathbf{Z} = \mathbf{Z}^+$ [17]. The relations between the matricant of (4) and the impedance matrix of (8) evaluated at cylindrical surfaces r, r_0 are easily deduced [17]

$$\mathbf{M}(r,r_0) = \begin{pmatrix} -\mathbf{Z}_2^{-1}\mathbf{Z}_1 & i\mathbf{Z}_2^{-1} \\ i\mathbf{Z}_3 - i\mathbf{Z}_4\mathbf{Z}_2^{-1}\mathbf{Z}_1 & -\mathbf{Z}_4\mathbf{Z}_2^{-1} \end{pmatrix},$$

$$\mathbf{Z}(r,r_0) = \begin{pmatrix} -i\mathbf{M}_2^{-1}\mathbf{M}_1 & i\mathbf{M}_2^{-1} \\ i\mathbf{M}_4\mathbf{M}_2^{-1}\mathbf{M}_1 - \mathbf{M}_3 & -i\mathbf{M}_4\mathbf{M}_2^{-1} \end{pmatrix}.$$
(9)

Introducing (9) into (7), we can relate the conditional impedance $\mathbf{z}(r)$ to the two-point impedance matrix $\mathbf{Z}(r,r_0)$ according to

$$\mathbf{z}(r) = \mathbf{Z}_3(\mathbf{Z}_1 - \mathbf{z}(r_0))^{-1}\mathbf{Z}_2 - \mathbf{Z}_4. \tag{10}$$

3. Piecewise uniform transverse isotropy

In this section we develop an approach suitable for piecewise uniform transversely isotropic cylinders by explicit calculation of the global impedance matrix **Z** of (8), from which the conditional impedance can be found using (10). The method is based on a recursive algorithm proposed by Rokhlin et al. [9] called the stiffness matrix method. The analysis in [9] was restricted to multilayered media in Cartesian coordinates, whereas the present method is applicable to cylindrically layered media of transverse isotropy. We will refer to Rokhlin and Wang [9] several times in this section to note the similarities and differences of the approaches.

Consider n > 1 layers of uniform transversely isotropic materials with the kth layer $r_{k-1} < r < r_k$, $k \in \overline{1,n}$, see Fig. 1. The explicit form of the local two-point impedance matrix of the kth layer is $\mathbf{Z}^k(r_k,r_{k-1})$ as defined by Eq. (B.9). Denote the global two-point impedance matrix for the cylinder between r_0 and r_k by $\mathbf{Z}^{\mathbf{K}} = \mathbf{Z}^{\mathbf{K}}(r_k,r_0)$. Our objective is the global two-point impedance matrix for the entire cylinder, $\mathbf{Z}(r_n,r_0) \equiv \mathbf{Z}^{\mathbf{N}}(r_n,r_0)$.

Consider first the two bordering layers between $r = r_0$ and $r = r_2$ and sharing the $r = r_1$ surface. Continuity of displacements and traction on the interface implies

$$\begin{pmatrix} \mathbf{V}_0 \\ -\mathbf{V}_1 \end{pmatrix} = -i \begin{pmatrix} \mathbf{Z}_1^a & \mathbf{Z}_2^a \\ \mathbf{Z}_3^a & \mathbf{Z}_4^a \end{pmatrix} \begin{pmatrix} \mathbf{U}_0 \\ \mathbf{U}_1 \end{pmatrix}, \tag{11a}$$

$$\begin{pmatrix} \mathbf{V}_1 \\ -\mathbf{V}_2 \end{pmatrix} = -i \begin{pmatrix} \mathbf{Z}_1^b & \mathbf{Z}_2^b \\ \mathbf{Z}_3^b & \mathbf{Z}_4^b \end{pmatrix} \begin{pmatrix} \mathbf{U}_1 \\ \mathbf{U}_2 \end{pmatrix}, \tag{11b}$$

where $\mathbf{Z}^a \equiv \mathbf{Z}^1(r_1,r_0)$, $\mathbf{Z}^b \equiv \mathbf{Z}^2(r_2,r_1)$. From the second row of Eq. (11a) and the first row of Eq. (11b), we have

$$\mathbf{U}_{1} = -(\mathbf{Z}_{4}^{a} + \mathbf{Z}_{1}^{b})^{-1}(\mathbf{Z}_{3}^{a}\mathbf{U}_{0} + \mathbf{Z}_{2}^{b}\mathbf{U}_{2}). \tag{12}$$

Introducing Eq. (12) into Eqs. (11a) and (11b), we define the impedance matrix $\mathbf{Z}^2(r_2, r_0)$ that relates the traction vector to the displacement vector on the inner $(r = r_0)$ and outer $(r = r_2)$ surfaces of the bilayer

$$\begin{pmatrix} \mathbf{V}_0 \\ -\mathbf{V}_2 \end{pmatrix} = -i\mathbf{Z}^2(r_2, r_0) \begin{pmatrix} \mathbf{U}_0 \\ \mathbf{U}_2 \end{pmatrix}, \tag{13}$$

where

$$\mathbf{Z}^{2}(r_{2},r_{0}) = \begin{pmatrix} \mathbf{Z}_{1}^{a} - \mathbf{Z}_{2}^{a} (\mathbf{Z}_{4}^{a} + \mathbf{Z}_{1}^{b})^{-1} \mathbf{Z}_{3}^{a} & -\mathbf{Z}_{2}^{a} (\mathbf{Z}_{4}^{a} + \mathbf{Z}_{1}^{b})^{-1} \mathbf{Z}_{2}^{b} \\ -\mathbf{Z}_{3}^{b} (\mathbf{Z}_{4}^{a} + \mathbf{Z}_{1}^{b})^{-1} \mathbf{Z}_{3}^{a} & \mathbf{Z}_{4}^{b} - \mathbf{Z}_{3}^{b} (\mathbf{Z}_{4}^{a} + \mathbf{Z}_{1}^{b})^{-1} \mathbf{Z}_{2}^{b} \end{pmatrix},$$
(14)

 $\mathbf{Z}_{i}^{a} = \mathbf{Z}_{i}^{1}$, $\mathbf{Z}_{i}^{b} = \mathbf{Z}_{i}^{2}$ and \mathbf{Z}_{i}^{k} (k = 1, 2, $i = \overline{1, 4}$) are given by Eqs. (B.9). Note that Eqs. (11a) and (11b) are similar, apart from a sign change, to Eqs. (19) and (20) in [9].

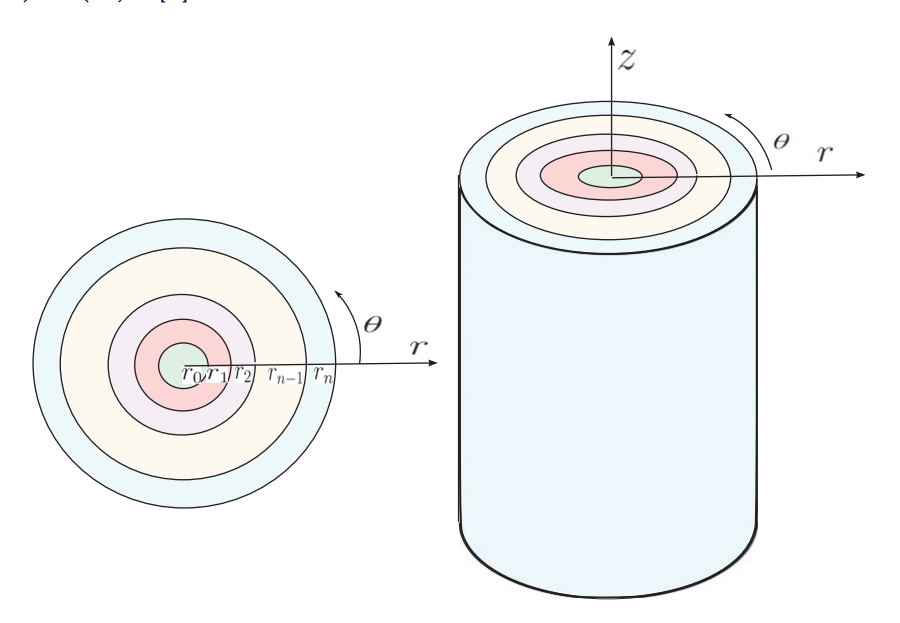


Fig. 1. A cylindrically anisotropic multilayered media is considered in the system of cylindrical coordinates. The media consists of *n* anisotropic layers with different densities and elasticity tensors in general.

Employing (13) recursively, the global impedance matrix $\mathbf{Z}^{\mathbf{K}}(r_k, r_0)$ for the cylinder between r_0 and r_k is obtained with 3×3 components

$$\mathbf{Z}^{\mathbf{K}} = \begin{pmatrix} \mathbf{Z}_{1}^{\mathbf{K}-1} - \mathbf{Z}_{2}^{\mathbf{K}-1} (\mathbf{Z}_{1}^{k} + \mathbf{Z}_{4}^{\mathbf{K}-1})^{-1} \mathbf{Z}_{3}^{\mathbf{K}-1} & -\mathbf{Z}_{2}^{\mathbf{K}-1} (\mathbf{Z}_{1}^{k} + \mathbf{Z}_{4}^{\mathbf{K}-1})^{-1} \mathbf{Z}_{2}^{k} \\ -\mathbf{Z}_{3}^{k} (\mathbf{Z}_{1}^{k} + \mathbf{Z}_{4}^{\mathbf{K}-1})^{-1} \mathbf{Z}_{3}^{\mathbf{K}-1} & \mathbf{Z}_{4}^{k} - \mathbf{Z}_{3}^{k} (\mathbf{Z}_{1}^{k} + \mathbf{Z}_{4}^{\mathbf{K}-1})^{-1} \mathbf{Z}_{2}^{k} \end{pmatrix},$$
(15)

where $\mathbf{Z}_{i}^{\mathbf{K}-\mathbf{1}}$ ($i=\overline{1,4}$) are the 3×3 sub-matrices of the matrix $\mathbf{Z}^{\mathbf{K}-\mathbf{1}}(r_{k-1},r_{0})$ for k-1 layers, \mathbf{Z}_{i}^{k} ($i=\overline{1,4}$) are the 3×3 sub-matrices of the matrix $\mathbf{Z}^{k}(r_{k},r_{k-1})$ for the kth layer, defined by Eq. (B.9). The global impedance matrix for the N-layered cylinder is obtained by using Eq. (15) (N-1) times.

The main differences between the present results and those of [9] are, first, that by construction the local \mathbf{Z}^k and global \mathbf{Z}^K two-point impedance matrices are Hermitian matrices. Second, the present results are valid for cylindrically layered structures, as compared with those of [9] which are for multilayered structures in Cartesian coordinates. Despite the differences, we note that the two-point impedance matrix \mathbf{Z}^k of Eq. (8) and the global two-point impedance matrix $\mathbf{Z}^K(r_k,r_0)$ are, apart from some sign differences, similar to the stiffness matrix \mathbf{K}^m and global stiffness matrix \mathbf{K}^M of Rokhlin and Wang [9].

4. Stable solution technique for general anisotropy

In this section we propose and demonstrate a stable numerical scheme for solving the conditional impedance matrix $\mathbf{z}(r)$ defined by (1) in the case of arbitrary radially dependent cylindrical anisotropy, i.e. density and elastic moduli are arbitrary functions of r: $\rho(r)$, $C_{ijk}(r)$.

4.1. Stability issues

Direct numerical integration of either (3) for the conditional impedance $\mathbf{z}(r)$ or (4) for the matricant $\mathbf{M}(r,r_0)$ is not a feasible strategy. The stiff nature of (4) leads to exponentially growing instabilities for \mathbf{M} . These become unavoidable at large values of n and/or kr for the elastic problem. On the other hand, singularities and numeric instabilities may form when Eq. (3) is integrated, which is a well-known issue for Riccati equations [18]. The singularities (poles) of the impedance matrix occur at finite values of r associated with traction-free modes for the given frequency. One can, in principle, avoid the singularity by switching to the differential equation for the inverse of the impedance: the admittance $\mathbf{A} = \mathbf{z}^{-1}$ [21, p. 136]. The admittance satisfies a Riccati differential equation, which follows from Eq. (3) as

$$\frac{d\mathbf{A}}{d\mathbf{r}} + i\mathbf{A}\mathbf{Q}_{3}\mathbf{A} + \mathbf{A}\mathbf{Q}_{4} - \mathbf{Q}_{1}\mathbf{A} + i\mathbf{Q}_{2} = 0. \tag{16}$$

However singularities again arise, this time corresponding to rigid modes. One could develop a numerical scheme that switches back and forth between integrating the impedance and admittance but since the locations of the singularities are not known in advance, and in practice they can be very close together, this does not offer a viable method. The curves shown in Fig. 2 exemplify the problem of singularities in the impedance. The appearance of the peaks in Fig. 2 indicates values of r beyond which accurate numerical solution cannot be obtained regardless of the step size in the integration scheme. The inability of such standard methods to obtain correct results was the motivation behind the proposed solution technique discussed next.

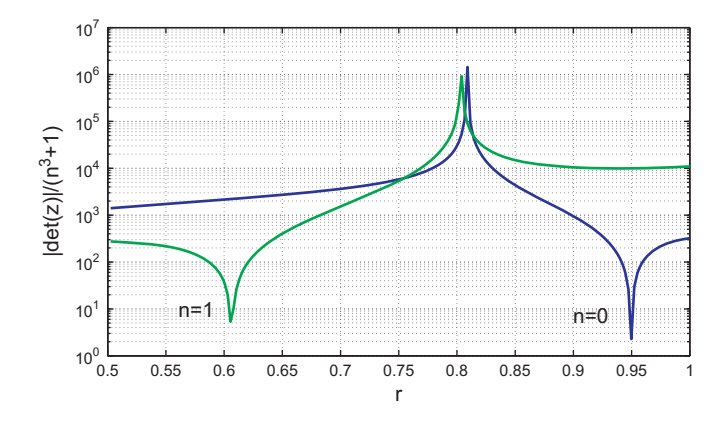


Fig. 2. Solid, aluminium cylinder integrated with 200 evenly spaced steps, using the fourth-order scheme of Section 4.4.2, from r=0.5 to r=1.0, with k_z =0 and ka=10. Plotted is the determinant of the upper left 2 × 2 sub-matrix of the 3 × 3 conditional impedance matrix normalized by n^3 + 1 vs. r. Where Eq. (B.7) was used for the initial impedance at r=0.5.

4.2. Möbius scheme

Numerical difficulties in integrating the matrix Riccati equations are well known and have been studied extensively. A procedure mentioned earlier for avoiding singularities is a generalization of the idea of switching, where one undergoes a change of variables, which is closely related to invariant embedding methods, see e.g. [22]. Here we follow a different approach, based on [18], which views the solution of the Riccati equation as a "Grassmanian flow" of m-dimensional subspaces (the impedance matrix) on a larger vector space of dimension 2m. The idea is to recast the equation for \mathbf{z} in the form of a forward marching scheme of step size h based on (7)

$$\mathbf{z}(r+h) = \mathbf{i}(\mathbf{M}_3 - \mathbf{i}\mathbf{M}_4\mathbf{z}(r))(\mathbf{M}_1 - \mathbf{i}\mathbf{M}_2\mathbf{z}(r))^{-1},\tag{17}$$

where $\mathbf{M} = \mathbf{M}(r+h,r)$. The key to the method is that \mathbf{M} can always be calculated in a stable manner for sufficiently small step size h. This approach is one of a class of methods called Möbius schemes, which by design are formulated on the natural geometrical setting of the larger vector space, in this case that of \mathbf{M} . Accordingly Möbius schemes are able to handle numerical instability and pass smoothly and accurately through singularities [18]. The method therefore combines both the matricant and the impedance, each of which is unstable when solved in a global sense separately.

4.3. Approximations for $\mathbf{M}(r+h,r)$

The Möbius scheme shifts the problem to that of finding approximations for $\mathbf{M}(r+h,r)$ accurate to some given order in h. The Peano series [20] of cascading integrals for the matricant is formally guaranteed to remain bounded for any h, but is numerically impractical. Our objective is to develop approximations for $\mathbf{M}(r+h,r)$ in the form

$$\mathbf{M}(r+h,r) = \mathbf{I}_{(2m)} + h\mathbf{M}^{(1)}(r) + \frac{h^2}{2!}\mathbf{M}^{(2)}(r) + \frac{h^3}{3!}\mathbf{M}^{(3)}(r) + \cdots,$$
(18)

where the terms $\mathbf{M}^{(2)}(r)$ do not require explicit integration schemes for their evaluation. Consider first the case of \mathbf{Q} sufficiently smooth. Then the identity

$$\mathbf{M}(r+h,r) = \mathbf{I}_{(2m)} + \int_0^h \mathbf{Q}(r+s)\mathbf{M}(r+s,r) \,\mathrm{d}s \tag{19}$$

may be written in the form of a series in powers of h by using (18) for the left member and a Taylor series evaluated at r for \mathbf{Q} in the integral

$$h\mathbf{M}^{(1)} + \frac{h^2}{2!}\mathbf{M}^{(2)} + \frac{h^3}{3!}\mathbf{M}^{(3)} + \dots = \int_0^h \left(\left[\mathbf{Q} + s\mathbf{Q}' + \frac{s^2}{2!}\mathbf{Q}'' + \frac{s^3}{3!}\mathbf{Q}''' + \dots \right] \times \left[\mathbf{I}_{(2m)} + s\mathbf{M}^{(1)} + \frac{s^2}{2!}\mathbf{M}^{(2)} + \dots \right] \right) ds, \tag{20}$$

with the argument r understood for all functions. Comparing equal orders of h^k in (20) implies

$$\mathbf{M}^{(1)}(r) = \mathbf{Q}(r),$$

$$\mathbf{M}^{(2)}(r) = \mathbf{Q}'(r) + \mathbf{Q}(r)\mathbf{M}^{(1)}(r),$$

$$\mathbf{M}^{(3)}(r) = \mathbf{Q}''(r) + 2\mathbf{Q}'(r)\mathbf{M}^{(1)}(r) + \mathbf{Q}(r)\mathbf{M}^{(2)}(r),$$

$$\mathbf{M}^{(4)}(r) = \mathbf{Q}'''(r) + 3\mathbf{Q}''(r)\mathbf{M}^{(1)}(r) + 3\mathbf{Q}'(r)\mathbf{M}^{(2)}(r) + \mathbf{Q}(r)\mathbf{M}^{(3)}(r),$$
(21)

etc. The matricant may now be found by employing (18). The series (21), while illustrative, is restricted to profiles that are analytically smooth functions of r. It is not suitable for piece-wise constant or piece-wise smooth profiles, which are of practical interest. Derivatives of the profile are therefore to be avoided if possible. In that sense, the approximation formed from Eqs. (18) and (21) is only valid to O(h), and the iterative scheme (17) shares the same accuracy.

An expansion accurate to second order can be obtained by using a Taylor series expansion evaluated at the midpoint [18]

$$\mathbf{Q}(r+s) \approx \mathbf{Q}\left(r+\frac{h}{2}\right) + \left(s-\frac{h}{2}\right)\mathbf{Q}'\left(r+\frac{h}{2}\right) + \left(s-\frac{h}{2}\right)^2\mathbf{Q}'' + O(s^3). \tag{22}$$

Substitution into (19) then gives, using (18)

$$\mathbf{M}^{(1)} = \mathbf{M}^{(2)} = \mathbf{Q}\left(r + \frac{h}{2}\right), \quad \mathbf{M}^{(3)} = \left(\mathbf{I}_{(2m)} + \frac{1}{2}\mathbf{Q}'\left(r + \frac{h}{2}\right)\right)\mathbf{M}^{(1)}. \tag{23}$$

This leads to an expansion up to $O(h^2)$ requiring only **Q** at a single position with no derivatives

TS 2nd:
$$\mathbf{M}(r+h,r) = \mathbf{I}_{(2m)} + h\mathbf{Q}\left(r + \frac{h}{2}\right) + \frac{h^2}{2}\mathbf{Q}^2\left(r + \frac{h}{2}\right) + O(h^3).$$
 (24)

The form of (24) suggests an alternative expression that is accurate to the same order

EXP 2nd(a):
$$\mathbf{M}(r+h,r) = \exp\left(h\mathbf{Q}\left(r+\frac{h}{2}\right)\right) + O(h^3). \tag{25}$$

Approximations (24) and (25), together with Eq. (17) each yield a second-order accurate Möbius scheme. EXP 2nd has the added feature that it is unimodular, and hence energy conserving. Detailed comparisons are provided in Section 4.6.

4.4. Lagrange interpolation expansions

We now consider Lagrange polynomial expansions for \mathbf{Q} in Eq. (19) in order to obtain higher order expressions without using derivatives of $\mathbf{Q}(r)$. The Lagrange polynomial of order n approximates $\mathbf{Q}(r+s)$ with the expression [23]

$$\mathbf{Q}(r+s) = \sum_{j=0}^{n} \mathbf{Q}(r+x_{j}h)L_{j}(\frac{s}{h}), \qquad L_{j}(x) = \prod_{l=0, l\neq j}^{n} \left(\frac{x-x_{l}}{x_{j}-x_{l}}\right), \tag{26}$$

where $x_j \in [0,1], j = 0,1,...,n$, are chosen points. Substituting into (20) and using the notation $\mathbf{Q}_{x_j} = \mathbf{Q}(r + x_j h)$ implies the sequence

$$\mathbf{M}^{(k)} = \left\{ \sum_{j=0}^{n} L_{j}^{(k)} \mathbf{Q}_{x_{j}} \right\} \mathbf{M}^{(k-1)}, \quad \mathbf{M}^{(0)} \equiv \mathbf{I},$$

$$L_{j}^{(k)} = k \int_{0}^{1} L_{j}(x) x^{k-1} \, dx, \qquad k = 1, 2, 3 \dots$$
(27)

Note that $\sum_{i=0}^{n} L_i^{(k)} = 1$. In the following subsections we derive expansions based on (26) for n=1 and n=3.

4.4.1. Two-point approximation: Halves

We approximate \mathbf{Q} with two points using (26) for n=1. In this case the integrals $L_j^{(k)}$ can be simplified with the result that

$$\mathbf{M}^{(k)} = \left\{ \sum_{j=0}^{1} L_j \left(\frac{k}{k+1} \right) \mathbf{Q}_{x_j} \right\} \mathbf{M}^{(k-1)}, \quad \mathbf{M}^{(0)} \equiv \mathbf{I}, \quad k = 1, 2, 3 \dots$$
 (28)

Taking equi-space points $x_0 = \frac{1}{4}$ and $x_1 = \frac{3}{4}$, yields

LP 2nd:
$$\mathbf{M}(r+h,r) = \mathbf{I}_{(2m)} + \frac{h}{2}(\mathbf{Q}_{1/4} + \mathbf{Q}_{3/4}) + \frac{h^2}{24}(\mathbf{Q}_{1/4} + 5\mathbf{Q}_{3/4})(\mathbf{Q}_{1/4} + \mathbf{Q}_{3/4}) + O(h^3).$$
 (29)

This again gives a Möbius scheme of second-order accuracy in h. It also suggests, by analogy with (25)

EXP 2nd(b):
$$\mathbf{M}(r+h,r) = \exp\left(\frac{h}{2}\mathbf{Q}_{3/4}\right) \exp\left(\frac{h}{2}\mathbf{Q}_{1/4}\right) + O(h^3).$$
 (30)

Note that the expansions (29) and (30) only agree with one another to first order, O(h).

4.4.2. Four-point approximation: Fourths

Taking four evenly spaced points to approximate \mathbf{Q} , $x_j = \frac{1}{8} + \frac{j}{4}$, j = 0,1,2,3, and using the symbolic algebra program Maple, yields

$$\begin{split} \boldsymbol{M}^{(1)} &= \frac{13}{48} \, \boldsymbol{Q}_{1/8} + \frac{11}{48} \, \boldsymbol{Q}_{3/8} + \frac{11}{48} \, \boldsymbol{Q}_{5/8} + \frac{13}{48} \, \boldsymbol{Q}_{7/8}, \\ \boldsymbol{M}^{(2)} &= \left(\frac{23}{720} \, \boldsymbol{Q}_{1/8} + \frac{67}{240} \, \boldsymbol{Q}_{3/8} + \frac{43}{240} \, \boldsymbol{Q}_{5/8} + \frac{367}{720} \boldsymbol{Q}_{7/8} \right) \boldsymbol{M}^{(1)}, \\ LP \ 4th : & \boldsymbol{M}^{(3)} &= \left(-\frac{1}{48} \, \boldsymbol{Q}_{1/8} + \frac{19}{80} \, \boldsymbol{Q}_{3/8} + \frac{7}{80} \, \boldsymbol{Q}_{5/8} + \frac{167}{240} \boldsymbol{Q}_{7/8} \right) \boldsymbol{M}^{(2)}, \\ \boldsymbol{M}^{(4)} &= \left(-\frac{23}{560} \, \boldsymbol{Q}_{1/8} + \frac{389}{1680} \, \boldsymbol{Q}_{3/8} - \frac{67}{1680} \, \boldsymbol{Q}_{5/8} + \frac{1427}{1680} \boldsymbol{Q}_{7/8} \right) \boldsymbol{M}^{(3)}. \end{split}$$

Substitution of these terms into (18) gives $\mathbf{M}(r+h,r)$ up to fourth-order accuracy. Interestingly, when more points were taken to evaluate \mathbf{Q} the numerical accuracy was not found to improve. This was tried with even spacings, using from five up to ten points. Finally, by analogy with (30) we define

EXP 2nd(c):
$$\mathbf{M} + (r+h,r) = \exp\left(\frac{h}{4}\mathbf{Q}_{7/8}\right) \exp\left(\frac{h}{4}\mathbf{Q}_{5/8}\right) \exp\left(\frac{h}{4}\mathbf{Q}_{3/8}\right) \exp\left(\frac{h}{4}\mathbf{Q}_{1/8}\right) + O(h^3),$$
 (32)

which, like (29) and (30), is consistent with the four-term Lagrange interpolation scheme (31) to first order.

4.5. Fourth-order Magnus integrator scheme

The Magnus integrator, created by Magnus [28], and further developed in [26] with a convergence proof and recurrence relations, is a method to approximate a solution to (4) with

$$\mathbf{M}(r+h,r) = \mathbf{e}^{\Omega}\mathbf{M}(r,r-h),\tag{33}$$

here we consider a fourth-order Magnus integrator scheme similarly done in [27] for the Helmholtz equation. We use the following definitions to march a solution forward in *r*:

$$\mathbf{M}(r+h,r) = e^{\Omega}\mathbf{M}(r,r-h),$$

$$MG 4th: \qquad \Omega = \frac{h}{2}(\mathbf{Q}_{(1)} + \mathbf{Q}_{(2)}) + \frac{\sqrt{3}h^2}{12}(\mathbf{Q}_{(2)}\mathbf{Q}_{(1)} - \mathbf{Q}_{(1)}\mathbf{Q}_{(2)}),$$

$$\mathbf{Q}_{(1)} = \mathbf{Q}(r+h(\frac{1}{2}-\frac{\sqrt{3}}{6})), \qquad \mathbf{Q}_{(2)} = \mathbf{Q}(r+h(\frac{1}{2}+\frac{\sqrt{3}}{6})).$$
(34)

As a fourth-order scheme the numerical precision of this method is very similar to that of the four-point Lagrange polynomial approximation (31), which is seen in the examples of the following section.

4.6. Numerical examples and convergence

In order to illustrate the convergence property of the different expansions proposed (exponential, Magnus, Taylor series, Lagrange polynomials), we consider a solid aluminium sample with properties $\rho=2.7~{\rm kg/m^3}$, $E=70~{\rm GPa}$, $G=26~{\rm GPa}$ and radius of r=1 and normalized these properties with respect to water for which $\rho=1.0~{\rm kg/m^3}$ and speed of sound in water $c=1.470~{\rm km/s}$. The numerical values reported were computed by implementing the Möbius scheme (17) and in the case of the Magnus integrator implementing (7), starting at r=0.5 with initial condition given by the explicit solution (B.7) from [17] and discussed in Section 4. In all examples we take $k_z=0$. Fig. 3 plots the difference in the determinant of the upper left 2×2 sub-matrix of the exact conditional impedance from (B.7), and that calculated by iterating (17) until r=1 is reached. The right hand side of Fig. 3 refers to the type of approximation used: Taylor Series (TS), Lagrange Polynomial (LP), Exponential (EXP), Magnus (MG), and to the accuracy order. Thus, LP 1st was calculated using Eq. (21), TS 2nd by (23), EXP (a) by (25), EXP (b) by (30), EXP (c) by (32), LP 2nd by (29), LP 4th by (31), MG 4th by (34), and LP 3rd was calculated using a Lagrange Polynomial with points $\{x_0,x_1,x_2\}=\{\frac{1}{6},\frac{1}{2},\frac{5}{6}\}$. Interestingly, the three EXP methods (Eqs. (25), (30) and (32)) gave similar results and were the best results for the fewest number of approximation points. Fig. 4 plots the difference in the upper 2×2 sub-matrices at r=1.0 vs. the number of steps used in the iteration from r=0.5 to r=1.0. As expected, the higher order schemes are more accurate and require fewer steps in the integration process to yield the same accuracy as a lower order scheme.

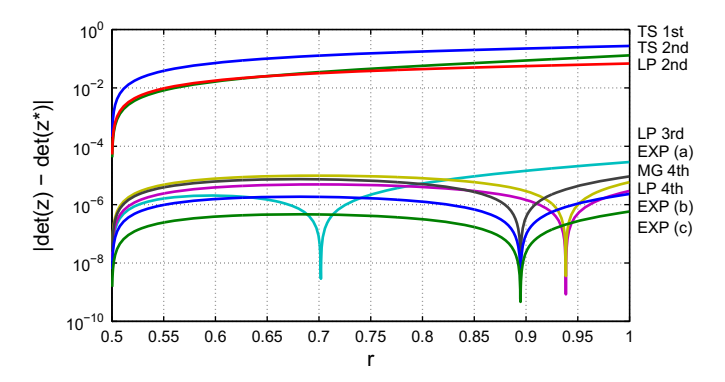


Fig. 3. Solid, aluminium cylinder integrated with 2000 evenly spaced steps from r=0.5 to r=1.0, with k_z =0, n=0 and ka=5. Plotted is the difference of the determinants of the upper left 2 × 2 sub-matrices of Eq. (B.7) and those calculated from Section 4. As noted in Section 4.6 the right hand side refers to the type and order accuracy, they are listed top to bottom as worst to best at r=1.

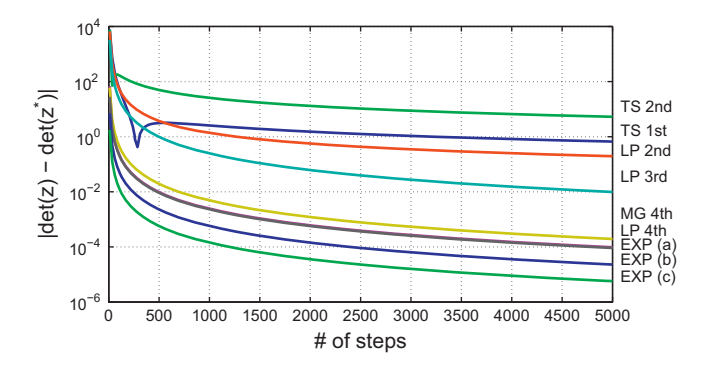


Fig. 4. Solid, aluminium cylinder integrated from r=0.5 to r=1.0, with $k_z=0$, n=0 and ka=2.5. Plotted is the difference of the determinants of the upper left 2×2 sub-matrices of Eq. (B.7) and those calculated from Section 4 at r=1 vs. # of steps.

5. Scattering example

In this section we explore the use of the impedance matrix by considering acoustic scattering from a solid aluminium cylinder immersed in water. Perpendicular plane wave incidence, i.e. k_z =0, in a uniform exterior fluid is considered with time harmonic dependence $e^{-i\omega t}$ henceforth omitted. The total radial stress and displacement fields in the surrounding fluid are

$$\sigma_{rr} = -Kk \sum_{n=-\infty}^{\infty} i^{n} (J_{n}(kr) + B_{n} H_{n}^{(1)}(kr)) e^{in\theta},$$

$$u_{r} = -\sum_{n=-\infty}^{\infty} i^{n} (J_{n}'(kr) + B_{n} H_{n}^{(1)}(kr)) e^{in\theta},$$
(35)

where r is the radial coordinate, K is the bulk modulus, k is the wavenumber, $H_n^{(1)}$ is the Hankel function of the first kind, and the coefficients B_n are to be determined [1]. We use the definition of the conditional impedance matrix, noted in Eq. (1), and write this statement for the innermost radial coordinate at r=b, for which we find the initial impedance matrix from Eq. (B.7), and for the outer surface at r=a where

$$\mathbf{V}(b) = -i\mathbf{z}_1\mathbf{U}(b), \quad \mathbf{V}(a) = -i\mathbf{z}_2\mathbf{U}(a). \tag{36}$$

The conditional impedance matrix, $\mathbf{z}_2 = \mathbf{z}(a)$, is found from the integration technique outlined in Section 4, or for transversely isotropic materials may be found directly using Eq. (B.7). Considering acoustic fluid in the exterior we write Eq. (36) for r=a in detail for which the shear stress, $\sigma_{r\theta}$, must be zero with

$$ia\begin{pmatrix} \sigma_{rr} \\ 0 \end{pmatrix} = -i\mathbf{z}_2 \begin{pmatrix} u_r \\ u_\theta \end{pmatrix} = -i \begin{pmatrix} p_1 & q_1 \\ p_2 & q_2 \end{pmatrix} \begin{pmatrix} u_r \\ u_\theta \end{pmatrix}. \tag{37}$$

Eliminating u_{θ} using the second row of Eq. (37) implies

$$ia\frac{\sigma_{rr}}{u_r} = \frac{i}{q_2}(q_1p_2 - q_2p_1) \equiv -iz_0.$$
 (38)

Using (35) and equating with (38) we find the scattering coefficient

$$B_n = -\frac{KkaJ_n(ka) + z_0J_n'(ka)}{KkaH_n^{(1)}(ka) + z_0H_n^{(1)'}(ka)}.$$
(39)

Numerical simulation was conducted for a solid aluminium cylinder with properties normalized with respect to water and with the total pressure field illustrated in Fig. 5. Fig. 6 shows both the total scattering cross-section σ_{tot} and the back-scattering amplitude $f(\pi)$, where the far field form function, $f(\theta)$, is

$$f(\theta) = \frac{2}{\sqrt{k}} \sum_{n=0}^{\infty} i^{2n-1} \epsilon_n B_n \cos n\theta, \tag{40}$$

where $\epsilon_0 = 1$ and $\epsilon_m = 2$ for m > 0. The total scattering cross-section is then

$$\sigma_{tot} = \frac{4\pi}{ka} \operatorname{Imag}(f(0)). \tag{41}$$

Fig. 6 closely matches the behavior of a similar analysis conducted in [24].

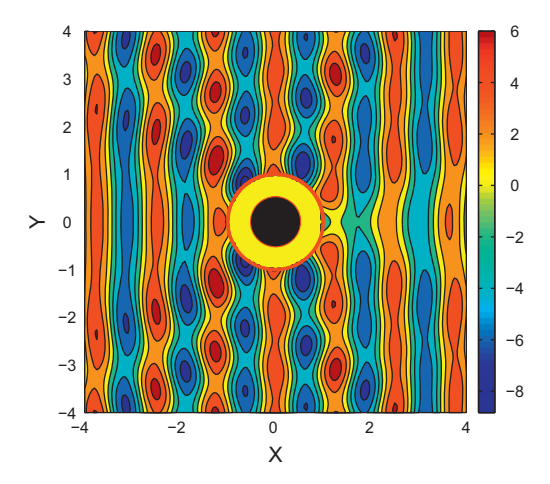


Fig. 5. Plotted pressure field described by Eq. (35) for an aluminium cylinder, integrated from r=0.5 to r=1.0 (area between the two red circles drawn) using the fourth-order scheme, Eq. (31), with 500 steps. The initial impedance at r=0.5 was found using Eq. (B.7). ka=5, k_z =0, and σ_{tot} = 2.468. (For interpretation of the references to color in this figure legend, the reader is referred to the web version of this article.)

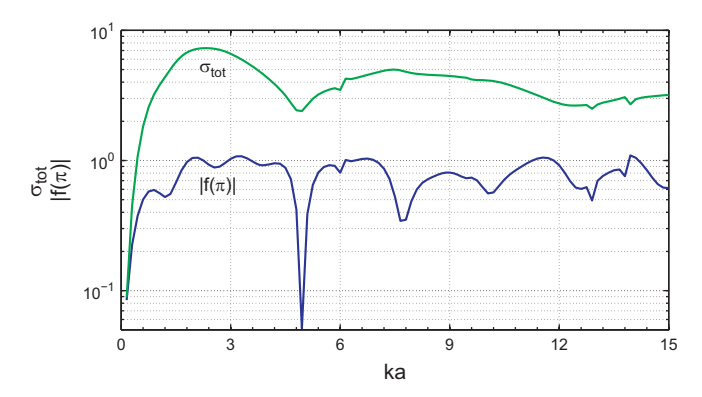


Fig. 6. Total scattering cross-section and backscattering amplitude plotted against non-dimensional frequency, ka. Aluminum cylinder with the same properties as listed in Fig. 5, integrated using the fourth-order scheme from r=0.5 to r=1.0 using 500 steps. The initial impedance at r=0.5 was found using Eq. (B.7).

6. Conclusion

Two computationally stable methods were considered to calculate the impedance matrix. Seeking solutions of 3D elasticity in the form of time-harmonic cylindrical waves, a matrix Riccati equation for the impedance matrix was formulated. Direct integration of the Riccati equation is numerically unstable, it leads to exponentially growing instabilities, which is inescapable at high frequency, large values of n, and layer thickness. We integrated the Riccati equation for the impedance matrix which has singularities along the real radial coordinate associated with traction free modes. To avoid instabilities we developed a new stable numerical scheme for cylindrically anisotropic structures that passes through these singularities by combining the impedance and matricant. This scheme evaluates the impedance matrix for continuous systems by integrating the Riccati equation over the thickness of each layer. Different expansion methods were considered and compared, it was noted that matrix exponential approximations yielded the best results.

An alternative method was developed to obtain the global impedance matrix for anisotropic, cylindrically layered media using the impedance matrix for each layer. The recursive formula to calculate the total two-point impedance was derived. The impedance matrix method was applied to obtain the total surface impedance matrix calculated recursively, layer by layer by employing the recursive formula N-1 times for an N layered system. In the case of more complex inhomogeneity and a large number of cylindrical layers, the recursive algorithm and the alternative integration technique are far superior to methods involving finite element analysis and can be performed with completely anisotropic materials.

Application of the impedance matrix simplifies the formulation of various scattering and boundary value problems for cylindrical structures. The impedance matrix can be applied to solve various acoustic and elastic scattering problems for arbitrarily layered cylindrical shells and solids. As an example acoustic scattering from a solid aluminium cylinder immersed in water was considered using the impedance matrix and compared with the literature. Plots of the total pressure field, form function and total scattering cross-section agree with previously published results.

Acknowledgments

This work was supported by the National Science Foundation and by the Office of Naval Research.

Appendix A. Cylindrically anisotropic media

The equilibrium equations of linear elastodynamics in cylindrical coordinates are [16]

$$(r\mathbf{t}_r)_r + \mathbf{t}_{\theta,\theta} + K\mathbf{t}_{\theta} + r\mathbf{t}_{z,z} = r\rho\ddot{\mathbf{u}}, \tag{A.1}$$

where $\mathbf{u} = (u_r, u_\theta, u_z)^T$ is the displacement vector, ρ is the mass density, \mathbf{t}_r , \mathbf{t}_θ , \mathbf{t}_z are the traction vectors, \mathbf{K} is the 3×3 matrix with $K_{12} = -1$, $K_{21} = 1$ and zero otherwise, T denotes transpose and a comma suffix denotes partial differentiation. Using the index notation $(r, \theta, z) \leftrightarrow (1, 2, 3)$ the stress–strain relationship is

$$\sigma_{ii} = C_{iikl} \varepsilon_{kl} \quad (= (\mathbf{t}_i)_i), \tag{A.2}$$

where the elastic stiffness tensor elements have the usual symmetries $C_{iikl} = C_{iikl} = C_{klii}$, and the notation of summation

over repeated indices is assumed. Combining the displacement strain equations in cylindrical coordinates with Eq. (A.2) the traction vectors are [16]

$$\begin{pmatrix} \mathbf{t}_r \\ \mathbf{t}_{\theta} \\ \mathbf{t}_z \end{pmatrix} = \begin{pmatrix} \hat{\mathbf{Q}} & \mathbf{R} & \mathbf{P} \\ \mathbf{R}^T & \hat{\mathbf{T}} & \mathbf{S} \\ \mathbf{p}^T & \mathbf{S}^T & \hat{\mathbf{M}} \end{pmatrix} \begin{pmatrix} \mathbf{u}_{,r} \\ r^{-1}(\mathbf{u}_{,\theta} + \mathbf{K}\mathbf{u}) \\ \mathbf{u}_{,z} \end{pmatrix}. \tag{A.3}$$

The form of the various matrices in (A.3) is, using Voigt notation for the moduli

$$\hat{\mathbf{Q}} = \begin{pmatrix}
C_{11} & C_{16} & C_{15} \\
C_{16} & C_{66} & C_{56} \\
C_{15} & C_{56} & C_{55}
\end{pmatrix}, \quad \hat{\mathbf{T}} = \begin{pmatrix}
C_{66} & C_{26} & C_{46} \\
C_{26} & C_{22} & C_{24} \\
C_{46} & C_{24} & C_{44}
\end{pmatrix}, \quad \hat{\mathbf{M}} = \begin{pmatrix}
C_{55} & C_{45} & C_{35} \\
C_{45} & C_{44} & C_{34} \\
C_{35} & C_{34} & C_{33}
\end{pmatrix},$$

$$\mathbf{R} = \begin{pmatrix}
C_{16} & C_{12} & C_{14} \\
C_{66} & C_{26} & C_{46} \\
C_{56} & C_{25} & C_{45}
\end{pmatrix}, \quad \mathbf{P} = \begin{pmatrix}
C_{15} & C_{14} & C_{13} \\
C_{56} & C_{46} & C_{36} \\
C_{55} & C_{45} & C_{35}
\end{pmatrix}, \quad \mathbf{S} = \begin{pmatrix}
C_{56} & C_{46} & C_{36} \\
C_{25} & C_{24} & C_{23} \\
C_{45} & C_{44} & C_{34}
\end{pmatrix}. \tag{A.4}$$

We consider cylindrically anisotropic media, illustrated in Fig. 1, for which the density, ρ , and elasticity tensor, \mathbf{C} , depend on the radial coordinate r. Solutions are sought in the form of time-harmonic cylindrical waves where the displacement and radial traction vectors are of the form

$$\mathbf{u} = \mathbf{U}^{(n)}(r)e^{\mathrm{i}(n\theta + k_z z - \omega t)}, \quad \mathrm{i} r \mathbf{t}_r = \mathbf{V}^{(n)}(r)e^{\mathrm{i}(n\theta + k_z z - \omega t)}. \tag{A.5}$$

where ω is the frequency, k_z is the axial wavenumber, and $n=0,1,2,\ldots$ is the circumferential number. Plugging (A.5) into (A.1) and (A.3) yields the state space representation [16] for the state vector $\boldsymbol{\eta}^{(n)}$ consisting of the displacement and radial traction vectors

$$\frac{\mathrm{d}}{\mathrm{d}r}\boldsymbol{\eta}^{(n)}(r) = \frac{\mathrm{i}}{r}\mathbf{G}(r)\boldsymbol{\eta}^{(n)}(r) \quad \text{with } \boldsymbol{\eta}^{(n)}(r) = \begin{pmatrix} \mathbf{U}^{(n)}(r) \\ \mathbf{V}^{(n)}(r) \end{pmatrix}. \tag{A.6}$$

The superscript (n) is omitted for the remainder of the paper. The 6×6 system matrix is [16]

$$i\mathbf{G} = \begin{pmatrix} \mathbf{g}^{(1)} & i\mathbf{g}^{(2)} \\ i\mathbf{g}^{(3)} & -\mathbf{g}^{(1)+} \end{pmatrix},$$
 (A.7)

where all terms depend on the radial coordinate, r, and the superscript + denotes the adjoint or conjugate transpose of a matrix. The 3×3 matrices in (A.7) are

$$\mathbf{g}^{(1)} = -\hat{\mathbf{Q}}^{-1}\tilde{\mathbf{R}} - ik_z r\hat{\mathbf{Q}}^{-1}\mathbf{P}, \quad \mathbf{g}^{(2)} = \mathbf{g}^{(2)T} = -\hat{\mathbf{Q}}^{-1},$$

$$\mathbf{g}^{(3)} = \mathbf{g}^{(3)+} = \tilde{\mathbf{T}} - \tilde{\mathbf{R}}^{+}\hat{\mathbf{Q}}^{-1}\tilde{\mathbf{R}} + ik_z r[\mathbf{P}^T\hat{\mathbf{Q}}^{-1}\tilde{\mathbf{R}} - \tilde{\mathbf{S}} - (\mathbf{P}^T\hat{\mathbf{Q}}^{-1}\tilde{\mathbf{R}} - \tilde{\mathbf{S}})^{+}] + r^2[k_z^2(\hat{\mathbf{M}} - \mathbf{P}^T\hat{\mathbf{Q}}^{-1}\mathbf{P}) - \rho\omega^2\mathbf{I}], \tag{A.8}$$

I is the 3×3 identity matrix, $^+$ indicates the Hermitian transpose, and

$$\tilde{\mathbf{R}} = \mathbf{R}\boldsymbol{\kappa}, \quad \tilde{\mathbf{S}} = \boldsymbol{\kappa}\mathbf{S}, \quad \tilde{\mathbf{T}} = \tilde{\mathbf{T}}^+ = \boldsymbol{\kappa}^+ \hat{\mathbf{T}}\boldsymbol{\kappa} \quad \text{with } \boldsymbol{\kappa} = \mathbf{K} + in\mathbf{I} \ (= -\boldsymbol{\kappa}^+).$$
 (A.9)

The system matrix, **G**, has the important symmetry [16] which follows from the form of (A.7):

$$\mathbf{G} = \mathbf{T}\mathbf{G}^{+}\mathbf{T} \quad \text{with } \mathbf{T} = \begin{pmatrix} \mathbf{0} & \mathbf{I} \\ \mathbf{I} & \mathbf{0} \end{pmatrix}. \tag{A.10}$$

The problem is now reduced to finding a solution to Eq. $(A.6)_1$ subject to appropriate boundary conditions. Next we introduce the matricant and impedance matrices based on solutions of $(A.6)_1$.

Appendix B. Impedance for uniform transverse isotropy

We consider transversely isotropic solids with the symmetry axis in the z-direction. The displacement vector may be decomposed using Buchwald's scalar potentials [19], the functions φ , γ and ψ

$$\mathbf{u} = \nabla \varphi + \nabla \times (\chi \mathbf{e}_z) + \left(\frac{\partial \psi}{\partial z} - \frac{\partial \varphi}{\partial z}\right) \mathbf{e}_z. \tag{B.1}$$

The general solution of the equilibrium equations for transverse isotropy is of the form $\{\varphi, \chi, \psi\} = \{\overline{\varphi}, \overline{\chi}, \overline{\psi}\} e^{i(n\theta + k_z z - \omega t)}$, where

$$\overline{\varphi} = R_{on}^{l} \frac{1}{k_{1}} f_{n}^{l}(k_{1}r) + \frac{1}{k_{2}} S_{on}^{l} f_{n}^{l}(k_{2}r),
\overline{\psi} = \frac{\kappa_{1}}{k_{1}} R_{on}^{l} f_{n}^{l}(k_{1}r) + S_{on}^{l} \frac{\kappa_{2}}{k_{2}} f_{n}^{l}(k_{2}r),
\overline{\chi} = -T_{on}^{l} \frac{1}{k_{3}} f_{n}^{l}(k_{3}r),$$
(B.2)

and R_{on}^l , S_{on}^l , T_{on}^l are unknown coefficients, $f_n^l(x)$ are cylindrical functions: $f_n^1(x) = J_n(x)$ for solutions that are regular at r = 0, $f_n^2(x) = Y_n(x)$ for real valued irregular solutions at r = 0, $f_n^3(x) = H_n^{(1)}(x)$ for outgoing (radiating) solutions, $f_n^4(x) = H_n^{(2)}(x)$ for ingoing solutions, where $J_n(x)$ is the Bessel function of the first kind; $Y_n(x)$ is the Bessel function of the second kind; $H_n^{(1,2)}(x)$ is the Hankel functions of the first and second kinds. The displacement field can be represented as a linear combination of any two of the four types of cylindrical functions $f_n^l(x)$ ($l = \overline{1,4}$). The wavenumbers k_1 , k_2 , k_3 , and non-dimensional numbers k_1 , k_2 are given by

$$k_{1,2}^{2} = \frac{a \mp \sqrt{a^{2} - b}}{2c_{11}c_{44}}, \quad k_{3}^{2} = \frac{\rho\omega^{2} - c_{44}k_{z}^{2}}{c_{66}}, \quad \kappa_{i} = \frac{c_{66}k_{3}^{2} - c_{11}k_{i}^{2}}{(c_{13} + c_{44})k_{z}} \quad (i = 1, 2),$$

$$a = (c_{11} + c_{44})\rho\omega^{2} + (c_{13}^{2} + 2c_{13}c_{44} - c_{11}c_{33})k_{z}^{2},$$

$$b = 4c_{11}c_{44}(\rho\omega^{2} - c_{33}k_{z}^{2})(\rho\omega^{2} - c_{44}k_{z}^{2}). \tag{B.3}$$

For isotropic material wavenumbers k_i , κ_i reduce to $k_1^2 = \omega^2 \rho/(\lambda + 2\mu) - k_z^2$, $k_2^2 = k_3^2 = \omega^2 \rho/\mu - k_z^2$, $\kappa_1 = 1$, $\kappa_2 = -k_2^2/k_z^2$. The displacement and traction vectors **U** and **V** of (A.5) are obtained in a matrix form for each n as

$$\mathbf{U}(r) = \sum_{l} \mathbf{X}^{l}(r) \mathbf{w}^{l}, \quad \mathbf{V}(r) = \sum_{l} \mathbf{Y}^{l}(r) \mathbf{w}^{l}, \quad \mathbf{w}^{l} = \begin{pmatrix} R_{on}^{l} \\ S_{on}^{l} \\ T_{on}^{l} \end{pmatrix}, \tag{B.4}$$

where the summation on l is over any two of the possible $l = \overline{1,4}$, and

$$\mathbf{X}^{l}(r) = \begin{pmatrix} f_{n}^{l}(k_{1}r) & f_{n}^{l}(k_{2}r) & -\frac{\mathrm{i}n}{k_{3}r}f_{n}^{l}(k_{3}r) \\ \frac{\mathrm{i}n}{k_{1}r}f_{n}^{l}(k_{1}r) & \frac{\mathrm{i}n}{k_{2}r}f_{n}^{l}(k_{2}r) & f_{n}^{l}(k_{3}r) \\ \frac{\mathrm{i}\kappa_{1}}{k_{1}}f_{n}^{l}(k_{1}r) & \frac{\mathrm{i}\kappa_{2}}{k_{2}}f_{n}^{l}(k_{2}r) & 0 \end{pmatrix},$$
(B.5)

$$\mathbf{Y}^{l}(r) = -i\mathbf{z}^{l}(r)\mathbf{X}^{l}(r), \tag{B.6}$$

and \mathbf{z}^l , $l = \overline{1,4}$, follows from [17]:

$$\mathbf{z}^{l}(r) = \begin{pmatrix} 2c_{66} & in2c_{66} & ik_{z}rc_{44} \\ -in2c_{66} & 2c_{66} & 0 \\ -ik_{z}rc_{44} & 0 & Z_{z} \end{pmatrix} + c_{0} \begin{pmatrix} \xi_{3}(y_{1}-y_{2}) & in(y_{1}-y_{2}) & i\xi_{3}(\xi_{1}-\xi_{2}) \\ -in(y_{1}-y_{2}) & \xi_{2}y_{1}-\xi_{1}y_{2} & n(\xi_{1}-\xi_{2}) \\ -i\xi_{3}(\xi_{1}-\xi_{2}) & n(\xi_{1}-\xi_{2}) & 0 \end{pmatrix},$$
(B.7)

$$Z_{z} = c_{44} \left(\frac{n^{2}(\xi_{1}y_{1} - \xi_{2}y_{2}) - \xi_{1}\xi_{2}\xi_{3}(y_{1} - y_{2})}{\xi_{3}(\xi_{2}y_{1} - \xi_{1}y_{2}) - n^{2}(y_{1} - y_{2})} \right), \quad y_{i} = \kappa_{i}r \quad (i = 1, 2),$$

$$c_{0} = \frac{c_{66}k_{3}^{2}r^{2}}{\xi_{3}(\xi_{2}y_{1} - \xi_{1}y_{2}) - n^{2}(y_{1} - y_{2})}, \quad \xi_{j} = k_{j}r \int_{f_{n}^{l}(k_{j}r)}^{l} \underbrace{(j = 1, 2, 3).}$$
(B.8)

The formula for \mathbf{X}^l follows by substituting the potentials (B.2) into Eq. (B.1) and agrees with Ahmad's results [25]. The derivation of the matrix $\mathbf{z}^l(r)$ can be found in [17]. Note that $\mathbf{z}^1(r)$ (l = 1) is the exact form of the conditional impedance of a solid cylinder, i.e. with material at r = 0 and hence bounded displacements there [17].

The explicit form of the two-point impedance matrix (see Eq. (8)) of a given transversely isotropic layer is

$$\mathbf{Z}^{k}(r_{k}, r_{k-1}) = \begin{pmatrix} \mathbf{Z}_{1}^{k} & \mathbf{Z}_{2}^{k} \\ \mathbf{Z}_{3}^{k} & \mathbf{Z}_{4}^{k} \end{pmatrix} = \begin{bmatrix} -\mathbf{Y}^{1}(r_{k-1}) & -\mathbf{Y}^{3}(r_{k-1}) \\ \mathbf{Y}^{1}(r_{k}) & \mathbf{Y}^{3}(r_{k}) \end{bmatrix} \begin{bmatrix} \mathbf{X}^{1}(r_{k-1}) & \mathbf{X}^{3}(r_{k-1}) \\ \mathbf{X}^{1}(r_{k}) & \mathbf{X}^{3}(r_{k}) \end{bmatrix}^{-1}.$$
(B.9)

Eq. (B.9), which defines the impedance matrix \mathbf{Z} , is similar to Eq. (7) of [9] (for the stiffness matrix \mathbf{K}), and the first and the second matrices on the right hand side of Eq. (B.9) are similar to the matrices \mathbf{E}_m^{σ} and $(\mathbf{E}_m^u)^{-1}$ in [9, Eqs. (5) and (3)]. One reason why we prefer to use the impedance matrix \mathbf{Z} rather than the stiffness matrix as in [9] is that the impedance is always Hermitian: $\mathbf{Z} = \mathbf{Z}^+$.

References

- [1] P.M. Morse, H. Feshbach, Methods of Theoretical Physics, vol. I, McGraw-Hill, New York, 1953.
- [2] L.M. Brekhovskikh, Waves in Layered Media, Academic, New York, 1960.
- [3] W. Huang, S. Brisuda, I. Rokhlin, Ultrasonic wave scattering from fiber-matrix interphases, Journal of the Acoustical Society of America 97 (1995) 807–817.
- [4] A. Sinclair, R. Addison, Acoustic diffraction spectrum of a SiC fiber in a solid elastic medium, *Journal of the Acoustical Society of America* 94 (1993) 1126–1135.
- [5] W. Huang, Y.J. Wang, S.I. Rokhlin, Oblique scattering of an elastic wave from a multilayered cylinder in a solid, *Journal of the Acoustical Society of America* 99 (1996) 2742–2754.

- [6] F. Honarvar, A.N. Sinclair, Scattering of an obliquely incident plane wave from a circular clad rod, Journal of the Acoustical Society of America 102 (1997) 41–48.
- [7] E.N. Thrower, The computation of the dispersion of elastic waves in layered media, Journal of Sound and Vibration 2 (1965) 210–226.
- [8] J.W. Dunkin, Computations of modal solutions in layered elastic media at high frequencies, Bulletin of the Seismological Society of America 55 (1965) 335–358.
- [9] S.I. Rokhlin, L. Wang, Stable recursive algorithm for elastic wave propagation in layered anisotropic media: stiffness matrix method, Journal of the Acoustical Society of America 112 (3) (2002) 822–834.
- [10] S.I. Rokhlin, L. Wang, A compliance/stiffness matrix formulation of general Greens function and effective permittivity for piezoelectric multilayers, *IEEE Ultrasonics, Ferroelectrics and Frequency Control.* 54 (4) (2004) 453–463.
- [11] H. Schmidt, F.B. Jensen, A full wave solution for propagation in multilayered viscoelastic media with application to Gaussian beam reflection at fluid-solid interfaces, *Journal of the Acoustical Society of America* 77 (1985) 813–825.
- [12] S.I. Rokhlin, W. Huang, Ultrasonic wave interaction with a thin anisotropic layer between two anisotropic solids: exact and asymptotic-boundary-condition methods, *Journal of the Acoustical Society of America* 92 (1992) 1729–1742.
- [13] A.N. Norris, A.L. Shuvalov, Elastic cloaking theorem, *Wave Motion* 49 (2011) 525–538.
- [14] A.N. Norris, Acoustic cloaking theory, Proceedings of the Royal Society A464 (2008) 2411-2434.
- [15] C.L. Scandrett, J.E. Boisvert, T.R. Howarth, Acoustic cloaking using layered pentamode materials, Journal of the Acoustical Society of America 127 (5) (2010) 2856–2864.
- [16] A.L. Shuvalov, A sextic formalism for three-dimensional elastodynamics of cylindrically anisotropic radially inhomogeneous materials, *Proceedings of the Royal Society A* 459 (2035) (2003).
- [17] A.N. Norris, A.L. Shuvalov, Wave impedance matrices for cylindrically anisotropic radially inhomogeneous elastic materials, Quarterly Journal of Mechanics and Applied Mathematics 63 (2010) 1–35.
- [18] J. Schiff, S. Shnider, A natural approach to the numerical integration of Riccati differential equations, SIAM Journal on Numerical Analysis 36 (5) (1999) 1392–1413.
- [19] V.T. Buchwald, Rayleigh waves in transversely isotropic media, Quarterly Journal of Mechanics and Applied Mathematics 14 (1961) 293-317.
- [20] M.C. Pease, Methods of Matrix Algebra, Academic Press, New York, 1965.
- [21] R. Bellman, G.M. Wing, An Introduction to Invariant Imbedding, Society for Industrial and Applied Mathematics, Philadelphia, USA, 1987.
- [22] H.B. Keller, M. Lentinim, Invariant imbedding, the box scheme and an equivalence between them, SIAM Journal on Numerical Analysis 19 (1982) 942–962.
- [23] J. P Berrut, L.N. Trefethen, Barycentric Lagrange interpolation, SIAM Review 46 (3) (2004) 501-517.
- [24] L. Flax, V.K. Varadan, V.V. Varadan, Scattering of an obliquely incident acoustic wave by an infinite cylinder, Journal of the Acoustical Society of America 68 (1980) 1832–1835.
- [25] F. Ahmad, A. Rahman, Acoustic scattering by transversely isotropic cylinders, International Journal of Engineering Science 38 (2000) 325-335.
- [26] A. Iserles, S.P. Norsett, On the solution of linear differential equations in Lie groups, *Philosophical Transactions: Mathematical, Physical and Engineering Sciences* 357 (1754) (1999) 983–1019.
- [27] Y.Y. Lu, A fourth-order Magnus scheme for Helmholtz equation, Journal of Computational and Applied Mathematics 173 (2) (2005) 247-258.
- [28] W. Magnus, On the exponential solution of differential equations for a linear operator, Communications on Pure and Applied Mathematics 7 (4) (1954) 649–673.